NOTICE
This version of the contribution has been accepted for publication, after peer review (when applicable) but is not the Version of Record and does not reflect post-acceptance improvements, or any corrections. The Version of Record is available online at: https://doi.org/10.1007/978-3-031-43075-6_18. Use of this Accepted Version is subject to the publisher's Accepted Manuscript terms of use:
https://www.springernature.com/gp/open-research/policies/accepted-manuscript-terms.

Multiplex Temporal Networks for Rapid Mental Workload Classification

Arya Teymourlouei[1], Joshua Stone[2], Rodolphe Gentili[3], and James Reggia[1]

[1] Department of Computer Science, University of Maryland, College Park MD 20742, USA
ateymo2@terpmail.umd.edu, reggia@umd.edu
[2] Department of Electrical and Computer Engineering, University of Maryland, College Park MD 20742, USA
jstone14@terpmail.umd.edu
[3] Department of Kinesiology, University of Maryland, College Park MD 20742, USA
roldolphe@umd.edu

Abstract. The automated classification of a participant's mental workload based on electroencephalographic (EEG) data is a challenging problem. Recently, network-based approaches have been introduced for this purpose. We seek to build on this work by introducing a novel feature extraction method for mental workload classification which uses multiplex networks formed from visibility graphs (VGs). The VG algorithm is an effective method for transforming a time series into a complex network representation. To analyze multivariate EEG time series, we construct multiplex temporal networks (MTNs), structures which contain the VGs of multiple EEG channels. We examine the tendency of layers in an MTN to share the same edges, referred to as layer entanglement. Using layer entanglement metrics as inputs, a support vector machine (SVM) classifier achieved an average 97% accuracy, 0.07 loss, and 99% F1 score in discrimination between two levels of cognitive workload based on EEG data. The findings presented here extend the findings from other recent studies that examined the prediction of mental workload. This work suggests that multiplex networks and layer entanglement can provide potential metrics for assessing mental workload with application to passive brain-computer interfaces.

Keywords: Multiplex network, layer entanglement, classification, mental workload, passive brain-computer interface (pBCI), electroencephalography (EEG).

1 Introduction

Cognitive computational neuroscience has rapidly progressed with the use of functional brain imaging techniques, such as EEG, functional magnetic resonance imaging, and positron emission tomography [1]. Researchers have investigated many aspects of human cognitive and cognitive-motor behavior including learning, working memory, motor planning, and mental workload [2, 3]. In particular, the study of mental workload has found applications in prosthetic devices [4], human-robot teaming [5], and passive brain-computer interfaces (pBCI) [6]. A pBCI makes use of brain dynamics to assess the cognitive state when performing a task. To ensure the usefulness of a robust pBCI, we require a method to classify the workload of a human user rapidly and accurately. In this research, we propose a novel method for workload prediction which studies the structural properties of multiplex temporal networks formed from EEG time series.

In recent work [7], we filtered EEG signals into five frequency ranges, and then transformed these signals into visibility graphs (VGs). The VG algorithm maps a univariate time series signal into a complex network. The random forest classifier that we used achieved a 92% accuracy. The approach in [7] differed from existing methods [6, 8, 9] in that the properties of the cortical signal were regionally extracted, as opposed to a representation that captures interactions between brain regions (known as functional connectivity).

The primary limitation of the work in [7] is that EEG classification was performed based on an entire 2.5-minute signal. A robust pBCI must be able to classify mental workload in a much shorter period of time. A recent EEG study on pBCI performed online classification with 30 seconds of signal [6]. Another pBCI study used a windowed-means approach, taking 8 windows of 0.05 seconds each [8]. The existing graph-based methodology is not able to accurately discriminate workload in such a time frame. Therefore, we expand on the work in [7] by proposing a new feature extraction method for mental workload classification. The methodology addresses the problem by using 5-second fragments of publicly available EEG data for classification.

Our methodology is to form a structure which contains the VGs of EEG channels, defined as a multiplex temporal network (MTN). In this structure, all graphs have identical nodes, because they correspond to the same time points on the signal. Each VG in the MTN is defined as a layer of the structure. In this work, we examine the tendency of layers of the MTN to share the same edges. That is, two corresponding nodes in two different layers have the same edge connecting them. The property of common edges between graphs in the MTN is defined as *layer entanglement*. Layer entanglement quantifies the similarity of layers in the MTN. We compute several metrics related to layer entanglement and use them as features for a support vector machine (SVM) classifier. We demonstrate here that the new method's mental workload classification accuracy is high even though it is based on much shorter 5 second EEG samples.

2 Background

2.1 Mental Workload

The EEG examination of mental workload has primarily been conducted through the assessment of regional cortical activity by means of spectral power. Previous work has observed that greater levels of mental workload led to an elevation of theta power (4-8 Hz) and an attenuation of alpha power (8-13 Hz) in various cortical regions [9]. More recently, methods which use connectivity to investigate the brain dynamics underlying mental workload have been proposed [10]. These approaches consider functional networks, where nodes are understood as brain regions, and edges between nodes signify a relationship between the regions. An example is in [10], which investigated the betweenness centrality of a multiplex brain network using wavelet bicoherence. The results of [10] found an increase in mental workload leads to stronger brain connectivity in higher frequencies.

2.2 Brain-Computer Interfaces

BCI is defined as a system that collects brain dynamics, performs analysis, and translates them into a state which is sent to an output device for use [11]. There are two types of BCI, passive and active. In active BCI, the user aims to control an external device (e.g., a computer cursor) by modifying their own cortical dynamics. Conversely, in pBCI the brain dynamics are recorded and processed to monitor specific user's mental states and determine what action should be taken accordingly. This work focuses on pBCI. One of the main challenges of pBCI is having a robust method for determining the brain state of the user. In the case of mental workload and EEG, the pBCI must be able to use the EEG signals to determine whether the user's mental workload level is high or low. This entire decoding process (from signal collection to quantification) must be executed quickly to avoid any delay in the user's state assessment when completing the task.

2.3 Multiplex Networks

Multiplex networks are structures which contain multiple graphs, where each graph contains the same nodes (only edges differ). Each graph is represented as a layer of the multiplex network. Such structures are useful for many problems in neuroscience. In this work, the construction of graphs from EEG time series is done by the VG algorithm. In previous work, networks were restricted to univariate time series [7]. Each VG accounts for the signal of one EEG channel. However, it is common in EEG applications to use more than one electrode. In the cases where multiple electrodes are used, EEG signals are a multivariate time series problem. It is often more powerful to represent a multivariate time series as one network. Each layer of the network represents one of the time series. Multiplex networks allow for a more in-depth analysis of the interactions between layers in the network.

A simple example of a multiplex network with two layers is presented in Fig. 1. Each layer in this toy example contains seven nodes where each node represents a single data point of an associated time series (not defined here). An edge between two nodes is formed by the criterion imposed by the natural VG algorithm. Each layer in the network represents one VG, associated with one EEG time series. Two nodes in both layers having the same edge signifies that the corresponding time series have a similar structure at the location of those data points. The corresponding points need not be identical, just similar enough that an edge is formed in both time series. Since this is a multiplex network, both layers share identical nodes, only intra-layer edges vary. In Fig. 1, we see the notion of coupling edges between the same nodes across different layers. We do not consider them further here because they lack the intuitive meaning in some other applications.

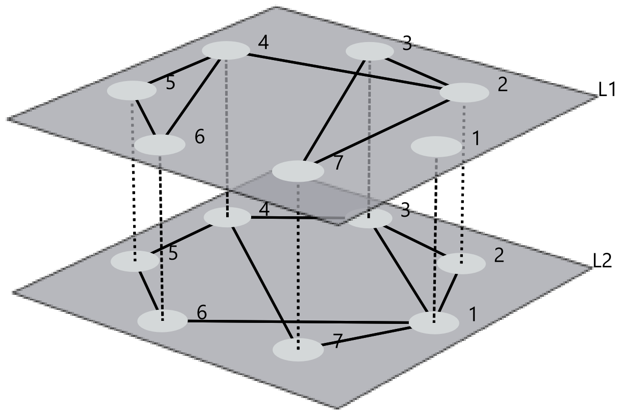

Fig. 1. A toy example of a multiplex network with two layers. Both layers of the network contain the same nodes, however edges in each layer can vary. Coupling edges (dashed lines) are presented for illustrative purposes, but our work does not consider them.

Many of the structural properties which are unique to multiplex networks exploit coupling edges. An example is the multiplex clustering coefficient, defined in [12]. However, another powerful structural property is the number of edges which layers share – commonly called edge overlap or layer entanglement. In our example in Fig. 1, we see several edges are common between the two layers. The set $S = \{\{5, 6\}, \{5, 4\}, \{3, 2\}\}$ contains the edges which are common between the two layers (therefore, entanglement of $S = 3$). Entanglement is a structural property which does not require coupling edges; therefore, it is suitable for this problem. It is a measure of the similarity between layers in a multiplex network. In the context of this methodology, layer entanglement quantifies the similarity of the VGs.

3 Methodology

The entire methodology is summarized in Fig. 2.

3.1 Mental Workload Task

In a pBCI, the user uses the assistance of a computer system to complete a task. The guidelines for systems, assistance, and tasks vary greatly by the application of the pBCI. In the context of mental workload, the task generally involves lower-demand versus higher-demand mental states. Experimental designs will follow this paradigm by creating task designs where one condition seeks to elicit low mental workload, and other(s) seek to generate high(er) workload. A popular study which follows this model is the Simultaneous Task EEG Workload (STEW) dataset [13]. The STEW dataset was collected under a low and high workload where participants did not execute any task and performed the Simultaneous Capacity Multi-Tasking task (SIMKAP), respectively [13]. SIMKAP is a cognitive task which involves completing several tasks at once. The tasks were checking for matching numbers, checking a telephone book, and checking a calendar. For each participant in STEW, data was collected as three minutes of at-rest and in-task channel data. After data collection, 30 seconds were removed from both conditions for each participant [13]. The total remaining time was 150 seconds.

In the STEW dataset, the mental workload of the participants was evaluated using EEG to determine cortical activity. There were 14 electrodes used in data collection, which were AF3, AF4, F3, F4, F7, F8, FC5, FC6, P7, P8, T7, T8, O1, and O2. To reduce computational complexity, in our study features were only calculated for 10 of the 14 channels. AF3, AF4, FC5, and FC6 were omitted. Raw EEG data was preprocessed with a Butterworth filter (1-40 Hz) and linear trends were removed. The EEG signals were segmented into 5-second windows. Then, the five typical frequency bands (δ, θ, α, β, γ) were extracted by means of band-pass filtering.

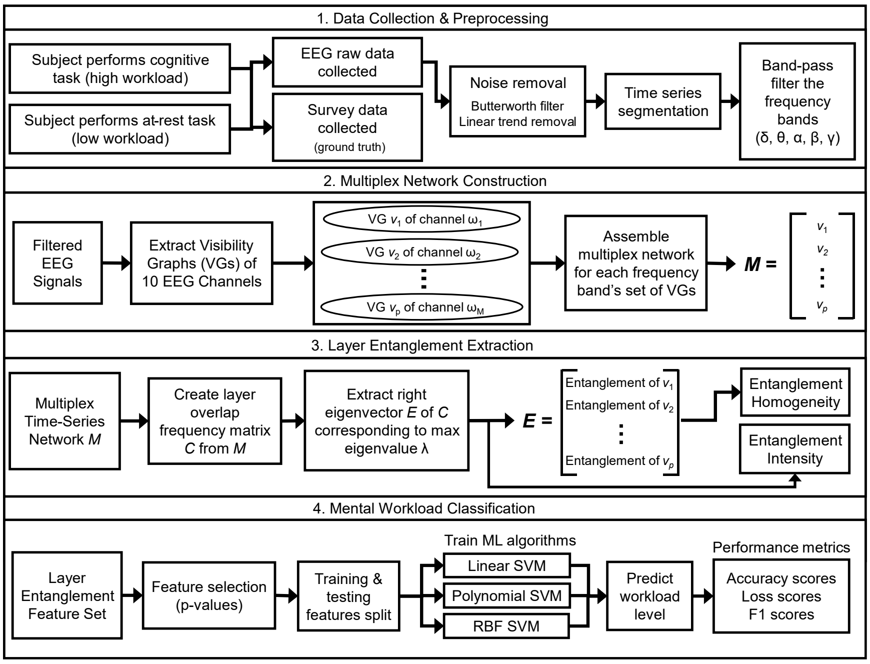

Fig. 2. Diagram of the methodology used for feature extraction. The collected EEG data is processed and prepared for transformation into graphs. The graphs for all channels are then assembled into an MTN, whose properties are extracted. These are fed to ML classifiers which then predict the level of workload taken by the EEG.

3.2 Network Construction

We use the natural VG algorithm to map an EEG signal into a network. VGs have been shown to effectively represent EEG signals of epilepsy [14], alcoholism [15], and mental workload [16]. The notion of visibility is intuitive. Two arbitrary samples on a time series have visibility if there is a straight line which connects them, which does not intersect any samples in between them. For a formal definition of visibility, we recall the original criterion from [17]. Consider two data points i and j, with associated values z_i and z_j, and an arbitrary point z_k. The data points i and j are represented as nodes in a graph, and are connected with a single edge if:

$$z_k < z_i + (z_j - z_i)\frac{k - i}{j - i} \qquad \forall\, k \in (i, j) \tag{1}$$

From this definition, we can construct VGs for each of the preprocessed EEG channels. To represent the VGs of multiple channels in one structure, a multiplex network is used. Let M be a multiplex network with 10 layers, one for the VG of EEG channel. Then, the VG of each channel is represented by a layer l in M, where $M = \{l_1, l_2, \ldots, l_{10}\}$. The channel corresponding to each layer is kept consistent. Therefore, l_1 always denotes the VG of the F3 channel, l_2 the F4 channel, and so on.

A layer l in M contains the nodes corresponding to the data samples of the EEG signal. For a temporal multiplex network, the *same* data points are considered for each layer. This is to ensure the VGs for the current multiplex network all correspond to the same time segment. For example, the first M formed will contain the samples from the first 5 seconds, for all layers.

3.3 Multiplex Network Analysis

As explained in the background, layer entanglement is a powerful structural property of multiplex networks. The definition of layer entanglement follows from [18]. Let $\boldsymbol{V}$ be the set of all nodes. Let $\boldsymbol{E} = \boldsymbol{V} \times \boldsymbol{V}$ be the set of all possible edges in the network, irrespective of layer. Let L refer to the number of layers in M. We introduce the matrix C, the layer overlap frequency matrix, defined as:

$$C = (c_{l,\,l'}) \tag{2}$$

where $(c_{l,\,l'})$ denotes an entry in the matrix. The non-diagonal elements are defined as:

$$(c_{l,\,l'}) = \frac{p_{l,\,l'}}{p_{l,\,l}} \tag{3}$$

where $p_{l,\,l'}$ refers to the number of edges that l and l' have in common, and $p_{l,\,l}$ refers to the number of edges in layer l. The diagonal elements of the matrix C are defined as:

$$(c_{l,\,l}) = \frac{p_{l,\,l}}{|\boldsymbol{E}|} \tag{4}$$

where $|\boldsymbol{E}|$ refers to the maximum possible number of edges in the layer l (this value would be the same for all layers, since all layers contain the same nodes). The layer entanglement vector is defined as the normalized, right eigenvector $\boldsymbol{e}$ associated with the *maximum* eigenvalue λ of the matrix C. An entry $\boldsymbol{e}_l$ in $\boldsymbol{e}$ is the entanglement of the layer l in M.

From the entanglement vector $\boldsymbol{e}$ and entanglement index λ, we can define several other measurements which extract more general observations of the multiplex network. These help to characterize the overall entanglement of a network (as opposed to $\boldsymbol{e}$, where the entanglement values of each layer are isolated). The entanglement homogeneity, denoted *EH*, is a cosine similarity. It measures the similarity of the entanglement of each layer [12]. It is defined as:

$$EH = \frac{\boldsymbol{n} \cdot \boldsymbol{e}}{||\boldsymbol{n}||\ ||\boldsymbol{e}||} \in [0, 1] \tag{5}$$

where $\boldsymbol{n} = [1, 1, \ldots, 1]$ refers to a vector of size L. Entanglement intensity is a measure of the amount of edge overlap in a multiplex network. The entanglement intensity, denoted *EI*, is defined as:

$$EI = \frac{\lambda}{L} \tag{6}$$

The layer entanglement vector, entanglement homogeneity, and entanglement intensity are computed for the constructed MTNs. These three metrics are used as the inputs to the ML classifier, which is explained in Section 3.5.

3.4 Feature Selection

The multiplex network metrics introduced in the previous section form the features of our classification procedure. However, redundant features were first removed using a feature selection process. The data was evaluated for normality using a Shapiro-Wilk test. Features which followed a normal distribution were then tested for significance using a paired t-test. Otherwise, significance was assessed with a Wilcoxon test. Features which showed a statistically significant difference ($p < 0.01$) between low and high mental workload were selected as input to the ML algorithm.

3.5 Classification

Features were fed to an SVM classifier, using a 5-fold cross-validation procedure. SVM is a popular ML model for neuroscience applications [15, 16]. In the results, we used three variants of SVM. All parameters are the same except for the kernel function. The linear function, polynomial (degree = 3) function, and radial-based function (RBF) are used. All classifiers are implemented in Scikit-Learn [19]. The regularization parameter varied from 0.92-0.98, depending on the SVM variant. We evaluate the performance of the SVM using three metrics: accuracy, loss, and F1. The accuracy is the percentage of correct predictions. Loss measures the magnitude of incorrect predictions. The F1 score is the harmonic mean of the precision and recall of the ML model [19].

The goal of a prediction model in pBCI is to classify the mental workload of one participant only. Cross-participant classification is also generally avoided due to differences between participants. For these reasons, we separate the classification procedure for each participant (n = 48) in the STEW data [13]. Each participant completed 150 seconds of at-rest and in-demand tasks. We segment the 150-second signal into 5-second windows. So, for each participant, there are 30 windows to classify. This is done for both low and high workload, so in total, it will be 60 windows per participant, or a total of 2880 samples total. 5-fold cross validation is performed during classification.

4 Results

In the results sections we focus on the layer entanglement metrics as a discriminator between low and high mental workload. The classification performance is assessed. Figures were generated with Python 3.10.4 using Matplotlib [20] and Seaborn [21] plotting packages.

4.1 Classification Performance

In this section we study the performance of three different SVM-based classifiers (variations of the kernel; linear, polynomial, radial-based function) trained to predict two levels of mental workload. All three figures presented in this section use point plots to illustrate the performance distribution for all STEW participants [21]. The position of the dot represents the mean value (accuracy, loss, or F1 score). The error bars indicate the standard error from the mean [21]. To reduce the Type I error, the false discovery rate (FDR; *Benjamini–Hochberg* procedure) was employed to correct for multiple comparisons. Fig. 3 presents the point plot for accuracy scores of the three ML classifiers.

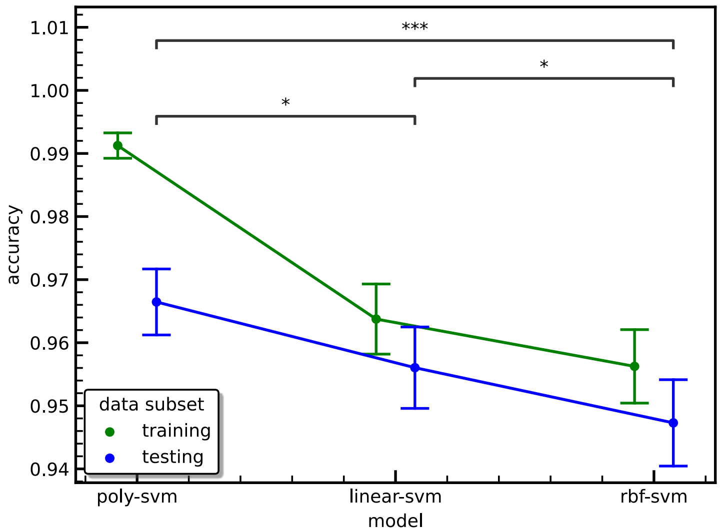

Fig. 3. Mean and standard error for the accuracy scores of three different SVM-based classifiers (variations of the kernel; linear, polynomial, radial-based function) to predict mental workload. Scores are computed for each participant (n=48). 5-fold cross-validation is used. Statistical significance is denoted as follows: *$p < 0.05$, ***$p < 0.001$.

Fig. 3 depicts the average accuracy of the SVM with the polynomial kernel is near 97% for testing data. The SVM with the linear kernel had an average testing accuracy of 95.6%. The SVM with the RBF kernel an average accuracy of 94.7% using testing data. There was a slightly significant decrease in testing accuracy between polynomial and linear SVM ($p = 0.012$) and linear and RBF SVM ($p = 0.034$). There was a more significant decrease in testing accuracy from polynomial to RBF SVM ($p = 0.0006$).

In Fig. 4, the mean loss scores for both training and testing data are shown to be below 0.1 for the polynomial SVM. The SVM with the linear kernel had an average testing loss of 0.25. The average testing loss was 0.20 for the SVM with RBF kernel. There was a statistically significant increase in testing loss between the polynomial and linear SVM ($p < 0.0001$) and polynomial and RBF SVM ($p < 0.0001$). A slight decrease in testing loss was also observed from linear to RBF SVM ($p = 0.042$).

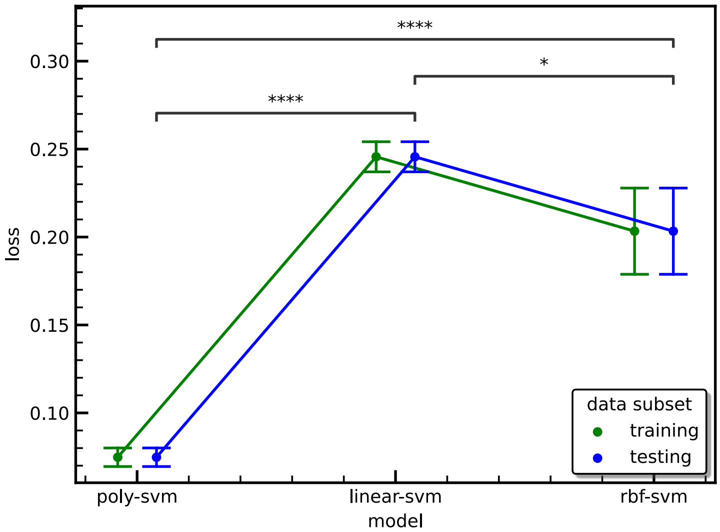

Fig. 4. Mean and standard error for the loss scores of three different SVM-based classifiers (variations of the kernel; linear, polynomial, radial-based function) to predict mental workload. Scores are computed for each participant (n=48). 5-fold cross-validation is used. Statistical significance is denoted as follows: *$p < 0.05$, ****$p < 0.0001$.

Fig. 5 depicts that the F1 scores were high for all three variants of the SVM. The SVM with the polynomial kernel had an average testing F1 of 99%, and for the linear kernel it was 96.3%. For the SVM trained with RBF kernel, the testing F1 score was 95.8%. For both training and testing data, the polynomial SVM had the least standard error. Comparison of F1 scores in testing data between linear and RBF SVM ($p = 0.032$) showed a slightly significant decrease. There was a much more significant decrease in testing F1 scores between polynomial and linear SVM ($p < 0.0001$) and polynomial and RBF SVM ($p < 0.0001$).

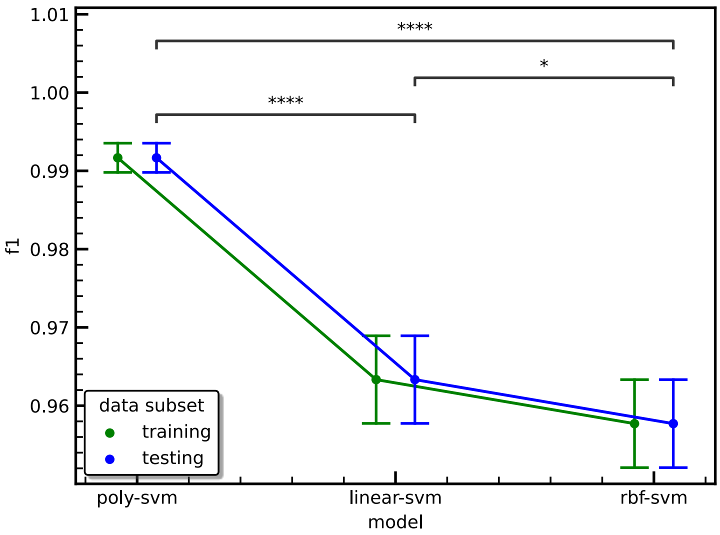

Fig. 5. Mean and standard error for the F1 scores of three different SVM-based classifiers (variations of the kernel; linear, polynomial, radial-based function) to predict mental workload. Scores are computed for each participant (n=48). 5-fold cross-validation is used. Statistical significance is denoted as: *p < 0.05, ****p<0.0001.

5 Discussion

In this work we have introduced a method for classifying between a low and high level of mental workload using a 5-second EEG time period and reported the results obtained using three variants of an SVM classifier. We demonstrated that our method performs well with three scoring metrics (accuracy, loss, F1). Overall, the results suggest the polynomial SVM had a significantly better performance than the other two models. The SVM with linear kernel also slightly outperformed the SVM with RBF kernel.

In this work, we addressed a major limitation of our previous work [7], that the processing time window for classification was too large, thus preventing any future pBCI applications which require small processing time periods. The results of this methodology extend previous studies that focused on predicting the changes in mental workload [6, 7, 15]. Critically, the proposed approach exceeded the performance of some previous prediction models. For example, the study in [6] had an average accuracy of 75%, whereas here we recorded 97%. In our own previous work, the best accuracy we achieved was 92% [7].

The purpose of this work is to enable rapid classification of mental workload, for use by pBCI. This has many clinical and biomedical applications. For example, it was previously suggested that in space exploration, workload is one of the factors impacted by long-term space habitation [22]. Another prior work suggested that environmental factors in space may be responsible for astronauts' difficulty in maintaining high cognitive performance [23]. Thus, pBCI may be able to serve as a countermeasure to the challenges faced by astronauts related to cognition and workload.

While our results are encouraging in terms of using the ML approach taken here for real-time pBCI applications, there are still some remaining challenges. One concern is the number of layers in the MTNs, which corresponds to the number of EEG channels used. The computational complexity of computing MTN-based metrics increases significantly when the number of layers becomes significantly large. Specifically, the computation of the number of overlapping edges between two layers in the MTN is an O(n) operation (n = number of edges). So, it may be beneficial to reduce the number of EEG channels processed for classification. However, this can lead to reduced ML performance. In addition, the layer entanglement metrics must be tested on other cognitive and cognitive-motor tasks to determine its effectiveness in other scenarios. In practical applications, it may prove useful to classify the mental workload into more than two classes.

Future efforts should focus on testing the use of layer entanglement as a biomarker to classify in real-time various levels of mental workload to verify whether it can be used in pBCI. Also, layer entanglement could be complemented by other EEG features resulting in multiple markers to provide a robust prediction model of mental workload. Beyond BCI applications, the method introduced here also can also serve in a more basic science context to examine the cognitive-motor mechanisms underlying mental workload to further understand the human adaptive behavior.

6 Acknowledgments

This work was supported by funding from the Maryland Space Grant Consortium and the University of Maryland College of Computer, Mathematical, and Natural Sciences Alumni Network.

References

1. Kriegeskorte, N., & Douglas, P. (2018). Cognitive computational neuroscience. *Nature Neuroscience*, *21*(9), 1148-1160.
2. Sylvester, J., Reggia, J., Weems, S., & Bunting, M. (2013). Controlling working memory with learned instructions. *Neural Networks*, *41*, 23-38.
3. Hauge, T., Katz, G., Davis, G., Huang, D., Reggia, J., & Gentili, R. (2021). High-level motor planning assessment during performance of complex action sequences in humans and a humanoid robot. *International Journal of Social Robotics*, *13*(5), 981-998.
4. Gaskins, C., Kontson, K., Shaw, E., Shuggi, I., Ayoub, M., Rietschel, J., ... & Gentili, R. (2018). Mental workload assessment during simulated upper extremity prosthetic performance. *Archives of Physical Medicine and Rehabilitation*, *99*(10), e33.
5. Edmonds, M., Gao, F., Liu, H., Xie, X., Qi, S., Rothrock, B., ... & Zhu, S. (2019). A tale of two explanations: Enhancing human trust by explaining robot behavior. *Science Robotics*, *4*(37).
6. Aricò, P., Borghini, G., Di Flumeri, G., Colosimo, A., Bonelli, S., Golfetti, A., ... & Babiloni, F. (2016). Adaptive automation triggered by EEG-based mental workload index: a passive

brain-computer interface application in realistic air traffic control environment. *Frontiers in Human Neuroscience*, *10*, 539.
7. Teymourlouei, A., Gentili, R., Reggia, J. (2023). Decoding EEG signals with visibility graphs to predict varying levels of mental workload. *Fifth Ann. Conf. on Info. Sciences and Systems, IEEE*.
8. Zander, T., Andreessen, L., Berg, A., Bleuel, M., Pawlitzki, J., Zawallich, L., ... & Gramann, K. (2017). Evaluation of a dry EEG system for application of passive brain-computer interfaces in autonomous driving. *Frontiers in Human Neuroscience*, *11*, 78.
9. Shaw, E., Rietschel, J., Shuggi, I., Xu, Y., Chen, S., Miller, M., ... & Gentili, R. (2019). Cerebral cortical networking for mental workload assessment under various demands during dual-task walking. *Experimental Brain Research*, *237*, 2279-2295.
10. Makarov, V., Zhuravlev, M., Runnova, A., Protasov, P., Maksimenko, V., Frolov, N., ... & Hramov, A. (2018). Betweenness centrality in multiplex brain network during mental task evaluation. *Physical Review E*, *98*(6), 062413.
11. Shih, J., Krusienski, D., & Wolpaw, J. (2012). Brain-computer interfaces in medicine. *Mayo Clinic Proceedings*, *87*(3), 268-279.
12. Battiston, F., Nicosia, V., & Latora, V. (2014). Structural measures for multiplex networks. *Physical Review E*, *89*(3), 032804.
13. Lim, W., Sourina, O., & Wang, L. (2018). STEW: Simultaneous task EEG workload data set. *IEEE Transactions on Neural Systems and Rehabilitation Engineering, 26*(11), 2106-2114.
14. Zhu, G., Li, Y., & Wen, P. (2012). Analysing epileptic EEGs with a visibility graph algorithm. *International Conf. on Biomedical Engineering and Informatics*, 432-436.
15. Zhu, G., Li, Y., Wen, P., & Wang, S. (2014). Analysis of alcoholic EEG signals based on horizontal visibility graph entropy. *Brain Informatics*, *1*(1), 19-25.
16. Zhu, G., Zong, F., Zhang, H., Wei, B., & Liu, F. (2021). Cognitive load during multitasking can be accurately assessed based on single channel electroencephalography using graph methods. *IEEE Access*, *9*, 33102-33109.
17. Lacasa, L., Luque, B., Ballesteros, F., Luque, J., & Nuno, J. (2008). From time series to complex networks: The visibility graph. *Proceedings of the National Academy of Sciences*, *105*(13), 4972-4975.
18. Škrlj, B., & Renoust, B. (2020). Layer entanglement in multiplex, temporal multiplex, and coupled multilayer networks. *Applied Network Science*, *5*(1), 1-34.
19. Pedregosa, F., Varoquaux, G., Gramfort, A., Michel, V., Thirion, B., Grisel, O., ... & Duchesnay, E. (2011). Scikit-learn: Machine learning in Python. *The Journal of Machine Learning Research*, *12*, 2825-2830.
20. Hunter, J. (2007). Matplotlib: A 2D graphics environment. *Computing in Science & Engineering*, *9*(03), 90-95.
21. Waskom, M. (2021). Seaborn: Statistical data visualization. *Journal of Open Source Software*, *6*(60), 3021.
22. De la Torre, G. (2014). Cognitive neuroscience in space. *Life*, *4*(3), 281-294.
23. Mhatre, S., Iyer, J., Puukila, S., Paul, A., Tahimic, C., Rubinstein, L., ... & Ronca, A. (2022). Neuro-consequences of the spaceflight environment. *Neuroscience & Biobehavioral Reviews*, *132*, 908-935.